Original Article

Institution of MECHANICAL ENGINEERS

Journal of MECHANICAL ENGINEERING SCIENCE

Proc IMechE Part C:
J Mechanical Engineering Science
2016, Vol. 230(18) 3304–3318

DOI: 10.1177/0954406215610361
pic.sagepub.com

SAGE

Load distribution of planetary roller screw mechanism and its improvement approach

Wenjie Zhang, Geng Liu, Ruiting Tong and Shangjun Ma

Abstract

A model of load distribution over threads of planetary roller screw mechanism (PRSM) is developed according to the relationships of deformation compatibility and force equilibrium. In order to make the applied load of PRSM uniformly distributed over threads, an improvement approach is proposed, in which the parameters of thread form of roller and nut are redesigned, and the contact conditions of roller with screw and nut are changed to compensate the axial accumulative deformation of shaft sections of screw and nut. A typical planetary roller screw mechanism is taken as example to analyze the load distribution, and the effects of installation configurations, load conditions and thread form parameters on load distribution are studied. Furthermore, the improvement approach is applied to the PRSM, and it is proved to be beneficial to reach uniform load distribution over threads.

Keywords

Planetary roller screw mechanism, load distribution, deformation compatibility relationship, thread form parameter, parameter redesign

Date received: 3 April 2015; accepted: 15 September 2015

Introduction

Planetary roller screw mechanism (PRSM) is a transmission device for converting rotary motion into linear motion or vice versa. As shown in Figure 1, the principal components of PRSM are screw A with multi-starts thread, a group of rollers B with single-start thread, nut C with internal multi-starts thread, two ring gears D fixed at both ends of the nut and meshed with the spur gears on both ends of rollers, and two retainers E which guarantee the rollers to be equally spaced around the screw. Threads of rollers mesh with threads of both screw and nut, which provides a quantity of contact points. Therefore, PRSM is of great advantage for working situation of large applied load. In addition, PRSM is capable of high transmission accuracy, high linear speed, high acceleration, and long service life. Owing to these advantages, PRSM has been widely used in maritime equipment,[1] electromechanical actuators,[2] machine tools,[3] and medical equipment.[4]

Earlier researches on PRSM mainly focused on parameters and kinematics,[5,6] optimal design,[7] stiffness and axial elastic deformation,[8,9] force and slip tendency,[10] and mode of failure.[11] Velinsky et al.[12] analyzed kinematics and transmission efficiency, which provided a fundamental basis to support applications of PRSM. Ma et al.[13] listed the necessary conditions of design parameters and then developed a model for calculating axial stiffness and frictional moment. Jones et al.[14] predicted the axial migration of the roller relative to the nut, and the results showed that the migration is due to the slip at the nut-roller interface, which is caused by a pitch mismatch between the spur-ring gear and the effective nut roller helical gear pairs. The nature of the contact between load transferring surfaces was investigated by Jones and Velinsky,[15] which provided a fundamental approach for further research of surface stresses, wear, and lifetime. Sokolov et al.[16] developed a model to investigate the force between working surfaces of the threads. Ma et al.[17] presented a frictional heat model, based on models of frictional moments of bearings and PRSM, in which factors of load distribution, lubricating oil, and the differential sliding of threads were taken into consideration. The results showed that the frictional heat rapidly decreased with the increase of contact angle of the threads.

Shaanxi Engineering Laboratory for Transmissions and Controls, Northwestern Polytechnical University, Xi'an, China

Corresponding author:
Geng Liu, Shaanxi Engineering Laboratory for Transmissions and Controls, Northwestern Polytechnical University, Xi'an 710072, China.
Email: npuliug@nwpu.edu.cn

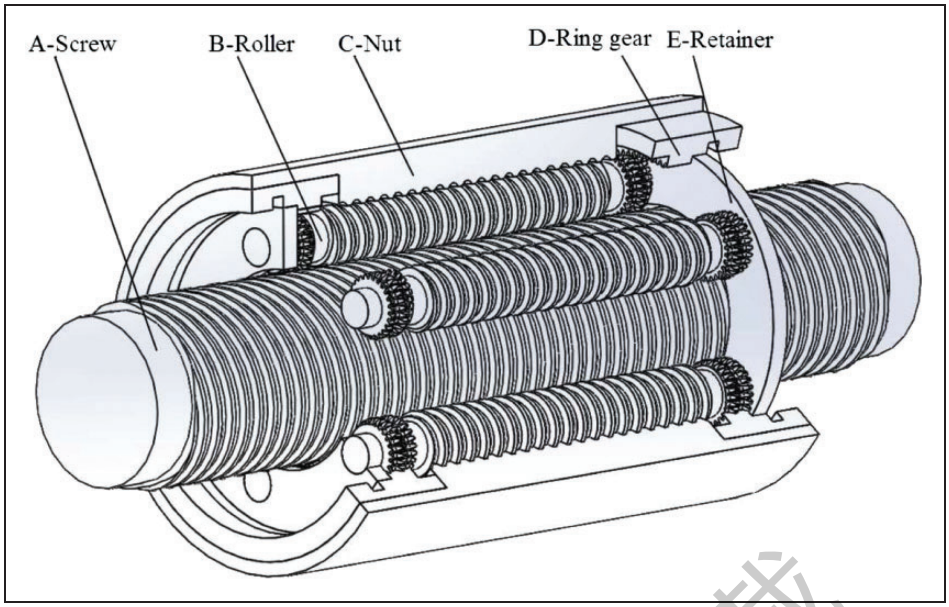

Figure 1. Planetary roller screw mechanism.

Load distribution over threads of PRSM is one of the most important characteristics of load bearing and has gradually attracted the attention of researches. Recently, Yang et al.[18] identified the roller as an object, and investigated load distribution and static rigidity. Deformations of shaft of screw, roller, and nut, and deformations of threads and contact points were considered. Load distribution was obtained by iterative computations from one to another thread of roller. Rys et al.[19] developed a model of load distribution between components in PRSM, which considered the deformations of rolling components as the deformations of rectangular volumes subjected to shear stresses. Contact deformation of threads and deformations of screw and nut cores were considered in the model. Jan's model can be used to analyze load distribution without detailed numerical calculations, and it is helpful to the preliminary design of PRSM. Ma et al.[17] investigated load distribution by regarding the thread of roller as a number of effective balls. By assuming that the load distributions on screw side and nut side are the same, load distribution was obtained from equilibrium conditions. The results were further used to develop a model of frictional moments. Jones et al.[20] constructed a stiffness model through direct stiffness method, which could be also used to predict the load distribution over the threads of individual components of PRSM. A spring system was constructed by considering the deformations of bodies, threads and contact points of screw, roller and nut. Based on the model, the design sensitivities of number of rollers and threads number of roller were studied. All of the above researches have helped researchers have a better understanding of the load distribution over threads of PRSM. However, load distribution is affected by many factors such as installation configurations, material parameters, structural parameters, thread form parameters, and so on. Existing models of load distribution over threads barely have an overall consideration of these factors.

In this paper, a new model is developed according to the deformation compatibility relationship of threads couples on screw and nut sides. In order to improve the nonuniform load distribution of PRSM, an improvement approach is proposed. Taking a typical planetary roller screw mechanism as example, the effects of installation configurations, load conditions and thread form parameters on load distribution are analyzed, and thread form parameters are redesigned to uniform the load distribution over threads.

Modeling

All of the threads of rollers will contact with the threads of screw and nut under applied load, and then deformations occur, which include shaft sections deformation, threads deformation, and contact deformation on contact points of threads. Load distribution over threads of PRSM is closely related to the above-mentioned three kinds of deformations. Corresponding to these three deformations, there are three kinds of stiffness. Among them, shaft section stiffness and contact stiffness are represented by coil springs and the thread stiffness is represented by leaf springs. Therefore, as shown in Figure 2, screw, roller, and nut of PRSM are decomposed into combinations of a group of coil springs and leaf springs. Here, a couple of contact threads are referred to as thread couple. The adjacent thread couples on screw or nut sides form a closed loop, in which the two contact points build a deformation compatibility relationship.

Following assumptions are made in this study: (1) Load distributions among rollers are the same. (2) There is no meshing clearance among threads. (3) Only the elastic deformation occurs under applied load.

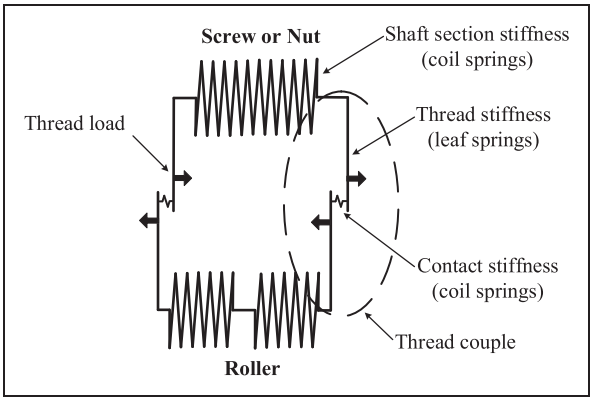

Figure 2. Decompose of threads in planetary roller screw mechanism.

Shaft section stiffness

Shaft section stiffness is defined as the tensile and compressive stiffness of the shaft sections between two adjacent bearing threads of screw, roller, and nut. For screw or nut, the shaft section stiffness is expressed as

$$k_{XS} = \frac{E_X \cdot A_X}{z \cdot P_X} \tag{1}$$

where P_X is the pitch of screw or nut, z is the number of rollers, E_X is the Young's modulus of screw or nut, A_X is the minimum cross-sectional area of shaft, the second subscript S which is the first letter of shaft denotes that the stiffness belongs to shaft section, and the subscript X can be denoted as S or N to represent screw or nut, respectively.

Roller meshes with screw and nut simultaneously, thus the shaft section stiffness of roller is the tensile and compressive stiffness of the shaft sections within half a pitch. It can be written as

$$k_{RS} = \frac{E_R \cdot A_R}{2 \times P_R} \tag{2}$$

where P_R is the pitch of roller threads, E_R is the Young's modulus of roller, A_R is the minimum cross-sectional area of roller, the second subscript S which is the first letter of shaft denotes that the stiffness belongs to shaft section, and the subscript R denotes roller.

Thread stiffness

As one of the three main deformations of PRSM, thread deformation occurs in axial direction on thread when load is applied on PRSM. In order to calculate thread deformation, formulae of Yamamoto[21] are used. Comparing the two situations of distributed load of screw fastener and point load of PRSM, it can be seen that the thread deformation of PRSM will be overestimated by using the formulae of Yamamoto.[21] However, all of the thread form parameters can be taken into consideration by the formulae of Yamamoto.[21] This will be favorable to investigate the effects of thread form parameters on load distribution and the results can help designers to choose reasonable value of thread form parameters. Therefore, the formulae in Yamamoto[21] are adopted in this paper to approximately evaluate the thread deformation of PRSM.

As shown in Figure 3, the thread deformation include bending deformation δ_1, shear deformation δ_2, deformation caused by root incline δ_3, deformation caused by root shear δ_4, and deformation caused by the radial component of thread load δ_5.

The thread forms of screw and nut are shown in Figure 3, where a is root width of thread form, b is thread thickness, c is crest width of thread form, h_f is dedendum of thread form, and θ is thread angle. The parameters of thread form of roller are defined in the same way. F_a is the axial component of thread load, and F_r is the radial component of thread load. The two components have the following relationship

$$F_r = F_a \cdot \tan(\theta/2) \tag{3}$$

where θ is thread angle, which is generally the same among screw, roller, and nut.

The bending deformation δ_1, shear deformation δ_2, deformation caused by root incline δ_3, and deformation caused by root shear δ_4 can be derived according to the following formulae[21]

$$\delta_1 = (1-\mu^2)\frac{3F_a}{4E} \cdot \left\{ \left[1 - \left(2 - \frac{b}{a}\right)^2 + 2\ln\left(\frac{a}{b}\right) \right] \cdot \cot^3(\theta/2) - 4\left(\frac{c}{a}\right)^2 \cdot \tan(\theta/2) \right\} \tag{4}$$

$$\delta_2 = (1+\mu)\frac{6F_a}{5E} \cdot \cot^3(\theta/2) \cdot \ln\left(\frac{a}{b}\right) \tag{5}$$

$$\delta_3 = \left(1-\mu^2\right)\frac{12c}{\pi E a^2} \cdot F_a \cdot \left(c - \frac{b}{2}\tan(\theta/2)\right) \tag{6}$$

$$\delta_4 = \left(1-\mu^2\right)\frac{2F_a}{\pi E}\left\{\frac{P}{a}\ln\left(\frac{P+a/2}{P-a/2}\right) + \frac{1}{2}\ln\left(\frac{4P^2}{a^2} - 1\right)\right\} \tag{7}$$

where μ is the Poisson's ratio of material, and E is the Young's modulus of material. Deformation caused by the radial component of thread load δ_5 is closely related to the structural parameters of thread, thus it is not identical for external and internal threads such as screw and nut. The external thread is identified as a cylinder whose diameter is d_p, and the internal thread is identified as a hollow cylinder whose external diameter is D_0 and internal diameter is d_p. δ_{5-e} and δ_{5-i} are the deformations caused by radial component of thread load of external and internal

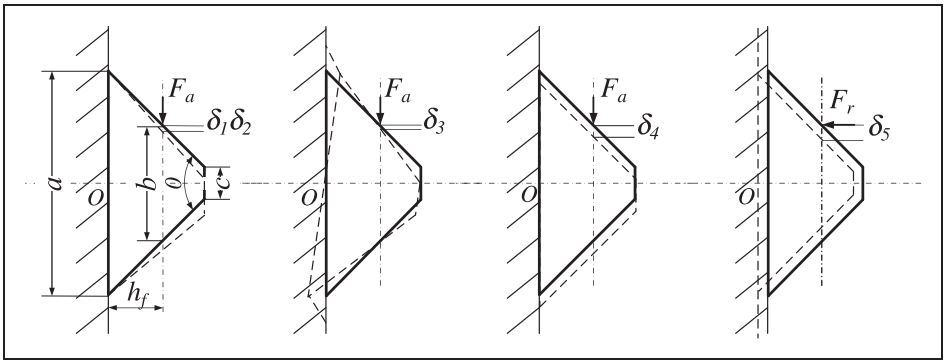

Figure 3. Various thread deformations of PRSM: (a) bending deformation δ_1 and shear deformation δ_2; (b) deformation caused by root incline δ_3; (c) deformation caused by root shear δ_4; (d) deformation caused by radial component of thread load δ_5.

threads, respectively. For external thread like screw and roller, δ_{5-e} can be expressed as[21]

$$\delta_{5-e} = (1-\mu)\frac{\tan^2(\theta/2)}{2}\cdot\frac{d_p}{P}\cdot\frac{F_r}{E} \tag{8}$$

For internal thread like nut, δ_{5-i} can be stated as[21]

$$\delta_{5-i} = \left(\frac{D_0^2+d_p^2}{D_0^2-d_p^2}+\mu\right)\frac{\tan^2(\theta/2)}{2}\cdot\frac{d_p}{P}\cdot\frac{F_r}{E} \tag{9}$$

Substitution of the parameters of screw, roller, and nut into equations (4) to (9) yields the total axial deformation of threads of screw, roller, and nut under thread load

$$\delta_{XT} = \delta_{X1}+\delta_{X2}+\delta_{X3}+\delta_{X4}+\delta_{X5} \tag{10}$$

Then the thread stiffness can be obtained as follows

$$k_{XT} = \frac{F_a}{\delta_{XT}} = \frac{F_a}{\delta_{X1}+\delta_{X2}+\delta_{X3}+\delta_{X4}+\delta_{X5}} \tag{11}$$

where k_{XT} is the thread stiffness, δ_{XT} is the total axial deformation of thread, the second subscript T which is the first letter of thread denotes that the stiffness belongs to thread, and subscript X can be denoted as S, R, or N to represent screw, roller, or nut, respectively.

Contact stiffness

According to Hertz contact theory, the contact deformation in normal direction at the contact point of thread couple on the screw side or nut side can be expressed as[22,23]

$$\delta_{XRC-normal} = \delta^*\left[\frac{3F_n}{2\Sigma\rho}\left(\frac{(1-\mu_R^2)}{E_R}+\frac{(1-\mu_X^2)}{E_X}\right)\right]^{2/3}\frac{\Sigma\rho}{2} \tag{12}$$

where $\delta_{XRC\text{-}normal}$ is contact deformation in normal direction on screw side or nut side, $\Sigma\rho$ is the summation of curvatures of two contact surfaces, δ^* is contact parameter that relates to $\Sigma\rho$, μ_R represents the Poisson's ratio of rollers, and μ_X represents the Poisson's ratio of screw or nut. F_n is the normal contact force between the two surfaces, i.e. the two contact threads.

In this study, deformations and loads are all considered in axial direction, so it is necessary for deformations and loads to be projected onto the axial direction. The relationship between the normal thread load and its axial component can be represented as[10]

$$F_n = F_a/(\cos\alpha_R\cdot\cos(\theta/2)) \tag{13}$$

The relationship between contact deformation and its axial component is the same with that of the contact force, which can be derived as

$$\delta_{XRC-axial} = \delta_{XRC-normal}\cdot\cos\alpha_R\cdot\cos(\theta/2) \tag{14}$$

In equations (13) and (14), α_R is helical angle of roller thread, θ is thread angle, and F_a is axial component of thread load. Thus the contact stiffness of threads on screw side or nut side can be calculated by

$$k_{XRC} = \frac{F_a}{\delta_{XRC-axial}} \tag{15}$$

Installation configuration

As shown in Figure 4, PRSM can be supported at the same ends of screw and nut or at the opposite ends, which are two installation configurations of PRSM.[20] Furthermore, PRSM has two contrary load conditions under applied load, in which screw and nut may withstand tension (abbreviated as "T") or compression (abbreviated as "C"). When PRSM bears applied load under different installation

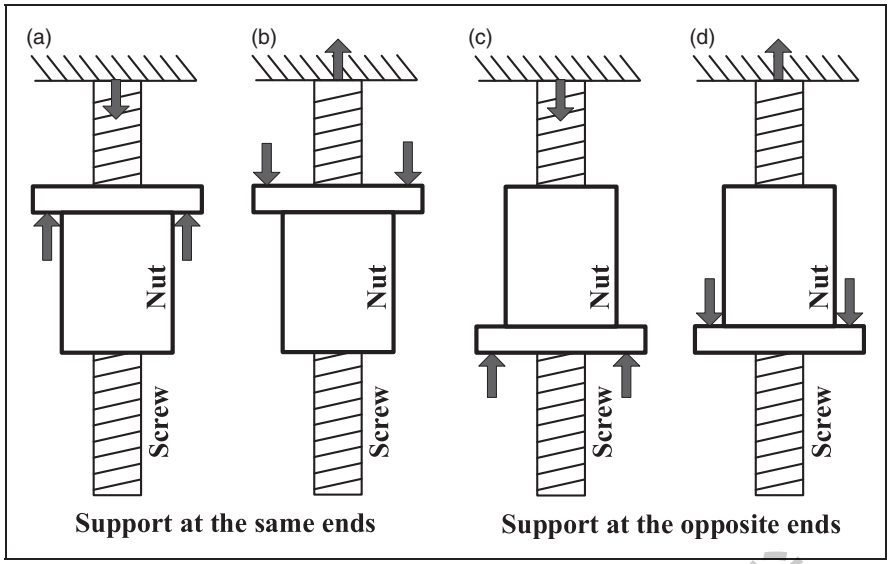

Figure 4. Different installation configurations and load conditions of PRSM[20]: (a) Screw-C, Nut-T; (b) Screw-T, Nut-C; (c) Screw-C, Nut-C; (d) Screw-T, Nut-T.

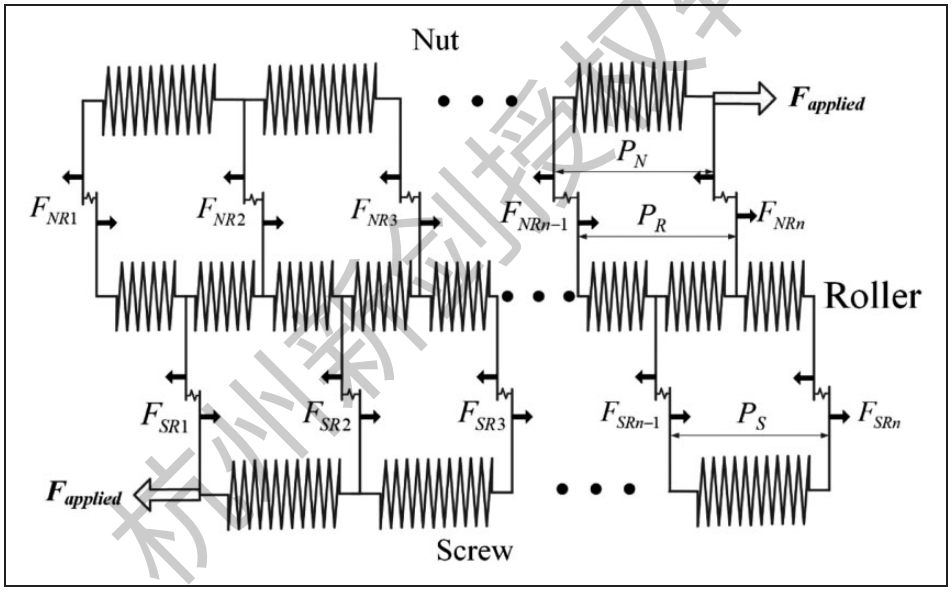

Figure 5. Load distribution model of PRSM.

configurations and load conditions, the deformations of components will change correspondingly, which lead to the change of load distribution. Consequently, the installation configurations and load conditions must be considered to analyze the load distribution of PRSM.

Load distribution model

Based on shaft section stiffness, thread stiffness and contact stiffness of screw, roller, and nut in PRSM, the load distribution model is developed. As shown in Figure 5, the shaft sections and contact points are represented by coil springs whose stiffness are equal to the shaft section stiffness and contact stiffness, respectively, and the threads are represented by leaf springs whose stiffness is equal to the thread stiffness.

The load distribution model of PRSM shown in Figure 5 is supported at the opposite ends of screw and nut, and is under "Screw-T, Nut-T" load condition, which is a case to exemplify the method to construct the model. The threads number of screw or nut meshing with roller is n, and it is $2n$ for roller because roller meshes with screw and nut simultaneously. F_{NRi} and F_{SRi} represent the axial components of thread load on the i-th thread couples on nut side and screw side, respectively. The solid arrows attached on leaf springs represent the direction of thread load. The i-th shaft section of screw, roller or nut is

defined as the shaft section between the i-th and $i+1$-th threads. $F_{applied}$ is the load shared on each roller, which is applied on screw and nut, and has the same magnitude and contrary directions. The PRSM reaches balance under the applied load. The adjacent couples of threads on screw side or nut side form a closed loop, in which the two contact points build a deformation compatibility relationship. The i-th closed loop is the portion which includes the i-th shaft section of screw or nut, and there are $2n-2$ closed loop in the model of PRSM shown in Figure 5.

Load on shaft section

The shaft sections of screw, roller and nut will bear axial load under the applied load of PRSM. The loads on shaft sections of screw and nut are the summation of thread loads on the threads from the corresponding shaft section to free end. Therefore, the loads on shaft sections of screw or nut get larger from free end to supported end, until it is equal to the applied load. It can be derived from Figure 5 that the axial load on the i-th shaft section of screw can be calculated by

$$F_{SSi} = F_{applied} - \sum_{j=1}^{i} F_{SRj} \quad i = 1, 2, \ldots, n-1 \tag{16}$$

where $F_{applied}$ is applied load shared on each roller of PRSM, and the axial load on the i-th shaft section of nut can be calculated by

$$F_{NSi} = \sum_{j=1}^{i} F_{NRj} \quad i = 1,\ 2, \ldots, n-1 \tag{17}$$

where F_{SSi} and F_{NSi} are the axial load on the i-th shaft section of screw and nut, respectively.

For the i-th shaft section of roller, the axial load can be expressed as the summation of thread loads on screw side and nut side as

$$F_{RSi} = \begin{cases} \sum_{j=0}^{\lfloor i/2 \rfloor} (F_{NRj} - F_{SRj}) + F_{NR(\lfloor i/2 \rfloor + 1)} \\ \quad i = 1, 3, \ldots, 2n-1 \\ \sum_{j=0}^{\lfloor i/2 \rfloor} (F_{NRj} - F_{SRj}) \\ \quad i = 2, 4, \ldots, 2n-2 \end{cases} \tag{18}$$

where F_{RSi} are the axial load on the i-th shaft section of roller, F_{SR0} and F_{NR0} are both equal to zero, and $\lfloor i/2 \rfloor = \text{floor}(i/2)$ is the largest integer not greater than $i/2$.

Deformation of shaft section

The axial deformation of shaft section can be obtained by the axial load applied on the corresponding shaft section. The axial deformation of the i-th shaft section of screw can be expressed as

$$\Delta l_{SSi} = \frac{F_{applied} - \sum_{j=1}^{i} F_{SRi}}{k_{SS}} \quad i = 1, 2, \ldots, n-1 \tag{19}$$

where $F_{applied}$ is applied load shared on each roller, and k_{SS} is the shaft section stiffness of screw. Similarly, the axial deformation of the i-th shaft section of nut can be described as

$$\Delta l_{NSi} = \frac{\sum_{j=1}^{i} F_{NRi}}{k_{NS}} \quad i = 1, 2, \ldots, n-1 \tag{20}$$

where k_{NS} is the shaft section stiffness of nut. For the i-th shaft sections of roller, the axial deformation can be expressed as

$$\Delta l_{RSi} = \begin{cases} \dfrac{\sum_{j=0}^{\lfloor i/2 \rfloor} (F_{NRj} - F_{SRj}) + F_{NR(\lfloor i/2 \rfloor + 1)}}{k_{RS}} \\ \quad i = 1, 3, \ldots, 2n-1 \\ \dfrac{\sum_{j=0}^{\lfloor i/2 \rfloor} (F_{NRj} - F_{SRj})}{k_{RS}} \\ \quad i = 2, 4, \ldots, 2n-2 \end{cases} \tag{21}$$

where k_{RS} is the shaft section stiffness of roller, F_{NRj} is the thread load of the j-th thread couple on nut side, and F_{SRj} is the thread load of the j-th thread couple on screw side.

Relationships of deformation compatibility and force equilibrium

In the closed loop formed by the adjacent threads couples on screw side or nut side, the two contact points satisfy the deformation compatibility relationship. Deformations within the closed loop and the deformation compatibility relationship are shown in Figure 6, in which the deformations are exaggerated for clarity.

In Figure 6, i is the number of thread, subscripts S, T, and C represent that the deformation Δl belongs to shaft section, thread and contact point, respectively. Taking the nut side as an example, the deformation compatibility relationship in the i-th closed loop can be represented as

$$P_N + \sum l_{Ni} = P_R + \sum l_{Ri} \tag{22}$$

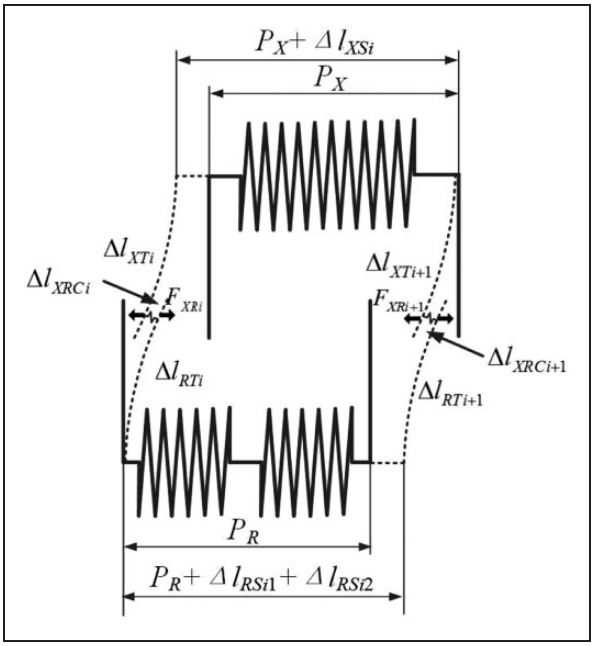

Figure 6. Deformation compatibility relationship of thread couples (exaggerated for clarity).

where Σl_{Ni} is the total deformation of nut within the i-th closed loop, and Σl_{Ri} is the total deformation of roller within the corresponding closed loop. Σl_{Ni} and Σl_{Ri} are respectively calculated by

$$\sum l_{Ni} = \Delta l_{NSi} + \Delta l_{NTi} + \Delta l_{NTi+1} + \Delta l_{NRCi} \tag{23}$$

$$\sum l_{Ri} = \Delta l_{RSi1} + \Delta l_{RSi2} + \Delta l_{RTi} + \Delta l_{RTi+1} + \Delta l_{NRCi+1} \tag{24}$$

where Δl_{NSi} is the axial deformation of the i-th shaft section of nut, Δl_{NTi} is the axial deformation of the i-th thread of nut, Δl_{NRCi} is the axial contact deformation of the i-th thread couple on nut side, and Δl_{RSi} is the axial deformation of the i-th shaft section of roller. Knowing that the nominal values of pitches of screw, roller, and nut are equal, i.e. $P_N = P_R = P_S$, and with the substitution of the shaft section stiffness, thread stiffness, and contact stiffness, equation (22) becomes as

$$\begin{aligned}&\frac{\sum_{j=1}^{i} F_{NRj}}{k_{NS}} + \frac{F_{NRi} - F_{NRi+1}}{k_{NT}} + \frac{F_{NRi}}{k_{NRC}} \\ &= \frac{\sum_{j=1}^{i} F_{SRj} - \sum_{j=1}^{i-1} F_{NRj}}{k_{RS}} \\ &\quad + \frac{F_{NRi+1}}{k_{RT}} - \frac{F_{NRi}}{k_{RS}} - \frac{F_{NRi}}{k_{RT}} - \frac{F_{NRi+1}}{k_{NRC}}\end{aligned} \tag{25}$$

The matrix form of equation (25) can be written as

$$\begin{bmatrix} \underbrace{\begin{matrix} k_{NS}^{-1} + 2\cdot k_{RS}^{-1} \\ \vdots \\ k_{NS}^{-1} + 2\cdot k_{RS}^{-1} \end{matrix}}_{i-1} \\ k_{NS}^{-1} + k_{NT}^{-1} + k_{NRC}^{-1} + 2\cdot k_{RS}^{-1} + k_{RT}^{-1} \\ -k_{NT}^{-1} - k_{RT}^{-1} - k_{NRC}^{-1} \\ \underbrace{\begin{matrix} 0 \\ \vdots \\ 0 \end{matrix}}_{n-i+1} \\ \underbrace{\begin{matrix} -2\cdot k_{RS}^{-1} \\ \vdots \\ -2\cdot k_{RS}^{-1} \end{matrix}}_{i-1} \\ -k_{RS}^{-1} \\ \underbrace{\begin{matrix} 0 \\ \vdots \\ 0 \end{matrix}}_{n-i} \end{bmatrix}^{T}_{2n\times 1} \cdot \begin{bmatrix} F_{NR1} \\ \vdots \\ F_{NRi-1} \\ F_{NRi} \\ F_{NRi+1} \\ F_{NRi+2} \\ \vdots \\ F_{NRn} \\ F_{SR1} \\ \vdots \\ F_{SRi-1} \\ F_{SRi} \\ F_{SRi+1} \\ \vdots \\ F_{SRn} \end{bmatrix} = 0 \tag{26}$$

Equation (26) can be derived from all the closed loops at both screw side and nut side. In addition, the summation of all of the axial components of thread loads on screw side or nut side is equal to the applied load shared on each roller of PRSM, which can be written as

$$\sum_{i=1}^{n} F_{XRi} = F_{applied} \tag{27}$$

Equation (27) can be transformed into matrix form. On nut side, it can be stated as

$$\left[\underbrace{1,\ 1,\ \cdots,\ 1}_{n},\quad \underbrace{0,\ 0,\ \cdots,\ 0}_{n}\right] \cdot [F_{NR1}, F_{NR2}, \ldots, F_{NRn}, F_{SR1}, F_{SR2}\cdots F_{SRn}]^T = F_{applied} \tag{28}$$

Similarly, on screw side, it can be expressed as

$$\left[\underbrace{0,\ 0,\ \cdots,\ 0}_{n},\quad \underbrace{1,\ 1,\ \cdots,\ 1}_{n}\right] \cdot [F_{NR1}, F_{NR2}, \ldots, F_{NRn}, F_{SR1}, F_{SR2}\cdots F_{SRn}]^T = F_{applied} \tag{29}$$

where $\mathbf{m} = [0, 0, \ldots, 0]_{1\times n}$, and $\mathbf{n} = [1, 1, \ldots, 1]_{1\times n}$. By combining equations (26), (28), and (29), the matrix equation of load distribution can be derived as

$$\begin{cases} \mathbf{K}\cdot\mathbf{f} = \mathbf{o}^T \\ [\mathbf{n}_{1\times n}|\mathbf{m}_{1\times n}]\cdot\mathbf{f} = F_{applied} \\ [\mathbf{m}_{1\times n}|\mathbf{n}_{1\times n}]\cdot\mathbf{f} = F_{applied} \end{cases} \tag{30}$$

where $\mathbf{K}$ is the matrix that presents the deformation compatibility relationship derived from all the closed loop, $\mathbf{o}$ is a row vector that all elements are 0, and $\mathbf{f} = [F_{NR1}, F_{NR2}, \ldots, F_{NRn}, F_{SR1}, F_{SR2}\cdots F_{SRn}]^T$ is the vector of thread loads.

Because of the nonlinearity of contact deformation, the contact stiffness on screw side and nut side, i.e. k_{SRC} and k_{NRC} vary with the contact deformation. Therefore, equation (30) is a nonlinear equation. In order to address this problem, following method is adopted to calculate the load distribution in this study. Firstly, assuming that the applied load is uniformly distributed over threads, the average thread load are taken as initial value to calculate the contact stiffness of each thread couples, which are all the same under the hypothesis. Then the obtained contact stiffness values are substituted into equation (30), and loads on each thread are further obtained. Then contact stiffness are calculated again by the new obtained thread loads. Finally, iterative computations are performed in this way and then the actual thread loads are obtained after k-th iterations. The error bounds is taken as $[F_{XRi}(k) - F_{XRi}(k-1)]/F_{XRi}(k-1) < 10^{-6}$.

Verification

In order to verify the model proposed above, the parameters of PRSM in Jones and Velinsky[20] are adopted to analyze the load distribution with the model developed in this study. The results are compared with those obtained in Jones and Velinsky,[20] as shown in Figure 7. In order to directly reflect the extent of non-uniform distributed of applied load over threads, load sharing coefficient is defined as the ratio of actual thread load to average thread load. The average thread load is defined as thread load when the applied load is uniformly distributed over threads, and the actual thread load is the results obtained by the model proposed above. Results show that the load distribution on screw side almost coincides with the result of Jones and Velinsky.[20] While on nut side, the results of this study are more uniform than Jones and Velinsky.[20] It is because smaller thread stiffness will make the applied load distribute more uniform over threads that discrepancy exists. Smaller thread stiffness exists because the deformation of thread caused by the radial components of thread load is taken into consideration in this model.

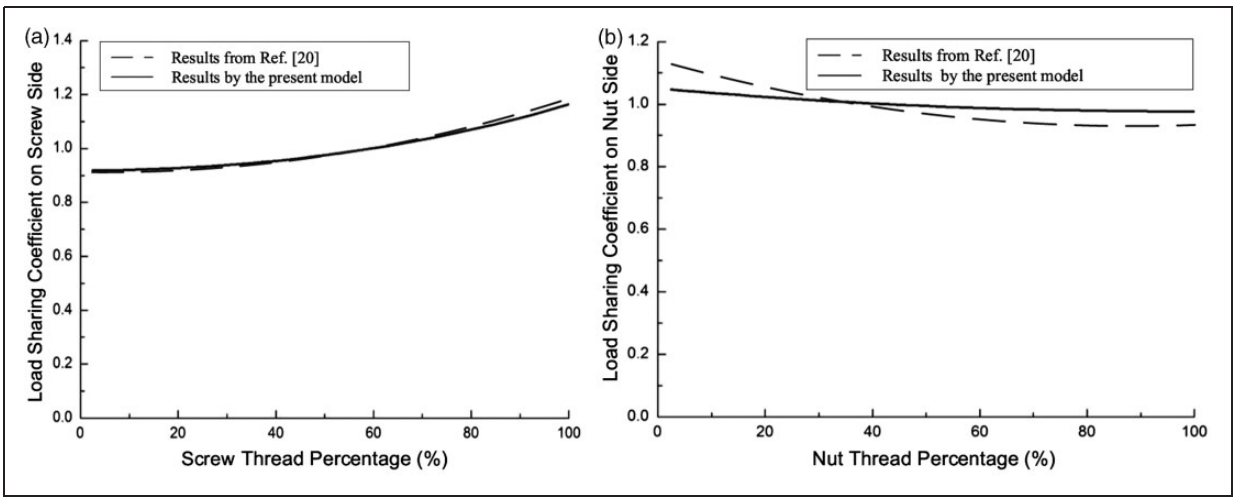

Figure 7. Comparison between results and Jones and Velinsky[20]: (a) screw side; (b) nut side.

Improvement approach to uniform the load distribution

Nonuniform distribution of applied load over threads is detrimental for load-bearing capacity and lifetime of PRSM, so it is important to improve the load distribution through design and manufacture approaches.

Under applied load, shaft sections of screw, roller, and nut will bear axial load, and axial deformations occur on shafts. The axial accumulative deformations of screw and nut are the main reasons for nonuniform load distribution. Thus compensating the axial accumulative deformation of screw and nut is a feasible approach to make the applied load distributed uniformly.

Axial accumulative deformation of shaft

From equations (19) to (21), the axial accumulative deformation of screw, roller and nut can be respectively calculated by

$$\Delta l_{sum-S} = \sum_{i=1}^{n-1} \frac{F_{applied} - \sum_{j=1}^{i} F_{SRj}}{k_{SS}} \tag{31}$$

$$\Delta l_{sum-N} = \sum_{i=1}^{n-1} \frac{F_{applied} - \sum_{j=i}^{n} F_{NRj}}{k_{NS}} \tag{32}$$

$$\Delta l_{sum-R} = \sum_{i=1}^{2n-1} \frac{\sum_{j=1}^{i-1} (F_{NRj} - F_{SRj}) + \sum_{t=1}^{n} F_{NRt}}{k_{RS}} \tag{33}$$

where $\Delta l_{sum\text{-}S}$, $\Delta l_{sum\text{-}N}$, and $\Delta l_{sum\text{-}R}$ are the axial accumulative deformation at the first thread of screw, nut, and roller, respectively.

Contact condition between threads

In order to make the applied load distribute more uniformly, the thread form parameters of screw, roller and nut are redesigned, in which the three thread components are meshing with different thread form and the initial contact conditions are changed. The improvement approach aims at making the threads with small thread load contact with each other before those with large thread load, when axial load is applied on PRSM. The clearances between threads allow the compensation of the axial accumulative deformation of screw and nut, so the load distribution becomes more uniform. Because the lead of screw is equal to the lead of PRSM, which is definitive, only the thread forms of roller and nut are redesigned according to that of screw. The screw side is adopted to illustrate the improvement approach which can also be applied to nut side.

When the thread forms of screw and roller are the same, the contact condition between them is showed in Figure 8, in which the screw and roller contact at the nominal diameter on both flanks. The relationship of thread form parameters can be represented by

$$e_S + e_R = P_S = P_R \tag{34}$$

where e_S and e_R are the thread thickness at nominal diameter of screw and roller, respectively.

When the thread forms of screw and roller are different from each other, the initial contact condition is changed, as shown in Figure 9. Thus equation (34) becomes

$$e_S + e_R + \xi + \varepsilon = P_S + \varepsilon_R = P_R \tag{35}$$

where ξ is the clearance between the thread couple, ε_R is the difference between the pitches of roller and screw.

Redesign of thread form parameters

To avoid interference and oversize clearance between threads, the pitch and thread thickness of roller need to be redesigned according to the thread number of roller and the pitch of screw thread. The feasibility of this redesign is guaranteed by the reality that the little change of the thread thickness almost has no influence on the thread stiffness and the load distribution.

When screw withstands tension, the pitch of roller should be designed slightly bigger than that of screw, so as to compensate the axial extension of screw shaft sections. According to the pitch of screw and thread number of roller, the thread thickness is redesigned to assure a fine contact condition.

As can be seen in Figure 10, the pitch of roller is bigger than that of screw. As a result when the n-th thread couple contacts, the other thread couples

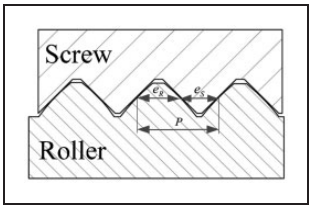

Figure 8. Mesh between threads of screw and roller.

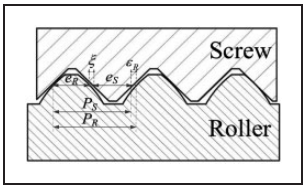

Figure 9. Contact between threads of screw and roller with different thread form.

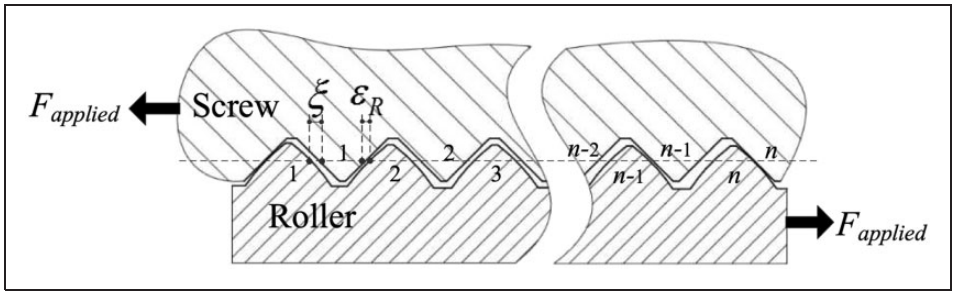

Figure 10. Redesign of thread form parameters when screw withstands tension (the initial contact condition before bearing load).

Table 1. Parameters of PRSM.

Parameter	Symbol	Value	Unit	Parameter	Symbol	Value	Unit
Nominal diameter of screw	d_S	24	mm	Applied load on PRSM	F	50,000	N
Nominal diameter of roller	d_R	8	mm	Applied load shared on each roller	$F_{applied}$	5000	N
Nominal diameter of nut	d_N	40	mm	Average thread load of roller threads	F_{ave}	250	N
External diameter of nut	d_{NW}	55	mm	Pitch of thread	P	2	mm
Starts of screw thread	n_S	5		Thread angle	θ	90	°
Starts of roller thread	n_R	1		Thread height	h	0.95	mm
Starts of nut thread	n_N	5		Root width of thread form	a	0.05	mm
Number of rollers	z	10		Thread thickness	b	0.85	mm
Number of roller threads	n	20		Crest width of thread form	c	0.05	mm

have clearances. To avoid unreasonable backlash between the threads caused by unequal pitch of screw and roller, the first thread couple of roller and screw is designed to contact on the opposite flank. The relationship of thread form parameters can be represented as

$$(n-1)\cdot P_R + e_R = (n-1)\cdot P_S + (P_S - e_S) \tag{36}$$

$$\varepsilon_R = \frac{P_S - e_S - e_R}{n-1} \tag{37}$$

where n is the threads number of roller, ε_R is the difference between pitch of screw and roller, and e_S and e_R are the thread thickness of screw and roller, respectively. In equations (35) to (37), ε_R, e_R, and ξ are all unknown, so it is necessary to search the relationship between ε_R and the axial accumulative deformation of screw. It can be seen in Figure 10 that the clearance between the threads of first thread couple, i.e. ξ is aiming to compensate the axial accumulative deformation of screw. The accumulative axial deformations of screw and roller at the first thread couple can be calculated by equations (31) and (33).

In addition, because of the nonuniform distribution of applied load, Hertz deformations on each thread are different from those when the load is uniformly distributed. Thus the difference of Hertz deformation must be taken into consideration. The Hertz deformations of threads under the average thread load and the actual thread load are denoted as δ_{ave} and δ_{act}, respectively.

Table 2. Material parameters of PRSM.

Part	Material	Young's modulus (MPa)	Poisson's ratio
Screw/Roller/Nut	GCr15	212×10^3	0.29

To appropriately compensate the axial accumulative deformation of components, the relationship among clearance of the first thread couple, the axial deformation of each component, and the Hertz deformation of first thread couple should be

$$\Delta l_{sum-S} - \Delta l_{sum-R} + \delta_{act} - \delta_{ave} - \xi = 0 \tag{38}$$

where $\Delta l_{sum\text{-}S}$ and $\Delta l_{sum\text{-}R}$ are the axial accumulative deformations at the first thread couple of screw and roller, respectively.

Based on the redesigned thread form shown in Figure 10, the n-th thread of roller will firstly contact with the thread of screw under applied load, while the other thread couples do not contact. After the deformations of shaft sections of screw and roller occur, the thread couples of screw and roller begin to contact in turn. The axial deformations of shaft sections of screw become larger when threads get closer to the support end of the screw. Thus the

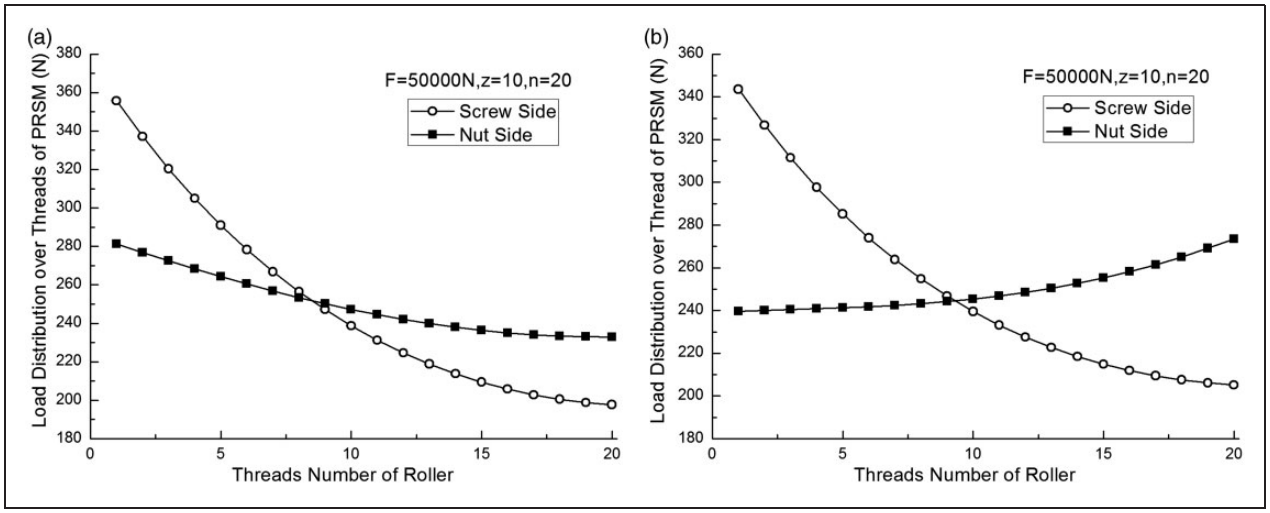

Figure 11. Load distributions under different installation configurations and load conditions: (a) Screw-C, Nut-T / Screw-T, Nut-C; (b) Screw-C, Nut-C / Screw-T, Nut-T.

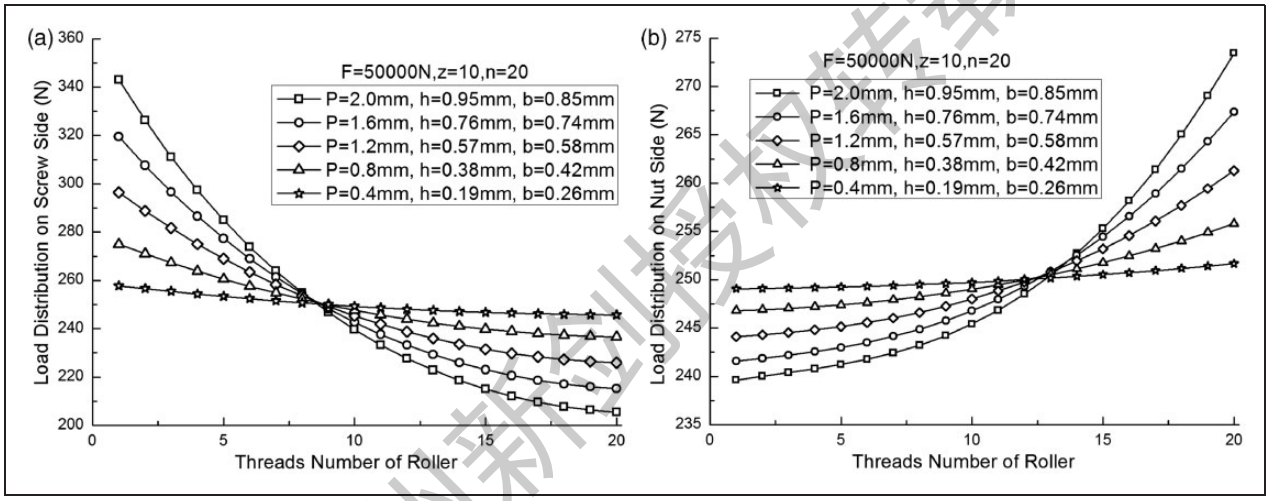

Figure 12. Effect of thread form on load distribution: (a) load distribution on screw side; (b) load distribution on nut side.

Table 3. Thread form parameters of roller and nut after redesign.

Thread form parameters of roller (redesigned refer to screw)					
P_R	2.0006 mm	P_S	2 mm	ξ	0.0114 mm
e_R	0.9886 mm	δ_{ave}	0.007 mm	$\Delta l_{sum\text{-}S}$	0.01098 mm
ε_R	0.0006 mm	δ_{act}	0.0086 mm	$\Delta l_{sum\text{-}R}$	0.000768 mm
Thread form parameters of nut (redesigned refer to roller)					
P_N	2.00035 mm	e_N	0.962 mm	ε_N	0.0002 5 mm

clearances between each couple of threads are designed to become larger from the free end to the support end. As a result, the clearance between threads will properly compensate the axial accumulative deformations of screw and roller, and then the applied load becomes more uniformly distributed over threads.

It should be noted that owing to the different direction of axial deformation, the redesign of thread form parameters is different under different load conditions. With the improvement approach shown in Figure 10, the applied load will distribute more uniformly under "Screw-T, Nut-T" load condition. However, it will aggravate the non-uniform distribution of applied load when PRSM is under "Screw-C, Nut-C" load condition. PRSM always has two load conditions under a certain installation configuration. Therefore, the improvement approach to uniform the

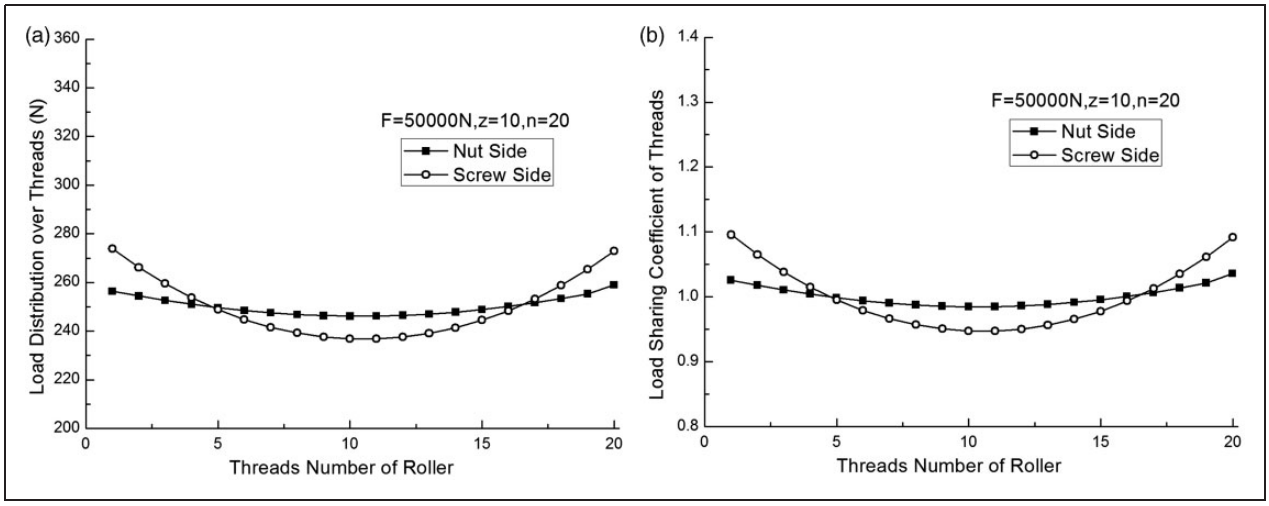

Figure 13. Load distribution after redesign parameters of thread form of roller and nut: (a) load distribution of PRSM; (b) load sharing coefficient of threads.

load distribution over threads is only suitable to the main load condition of PRSM.

Example

A typical planetary roller screw mechanism is taken as example to investigate the effects of installation configurations, load conditions and thread form parameters on load distribution. After that, the thread form parameters of roller and nut are redesigned to uniform the load distribution of PRSM. Detailed parameters of PRSM are listed in Tables 1 and 2.

Effect of installation configuration and load condition

Load distributions of PRSM under different installation configurations and load conditions (as shown in Figure 4) are investigated, and the results are shown in Figure 11.

Figure 11 shows that load distributions over threads of PRSM are different under different installation configurations, but they are the same when PRSM is under different load conditions with a certain installation configuration. When PRSM is installed at the opposite ends of screw and nut, the variation tendency of thread loads on nut side and screw side are contrary, while the variation tendencies are the same when installed at the same ends. Load distribution on nut side is always more uniform than that of screw side. The differences of load distribution between screw and nut sides are caused by two reasons. Firstly, different shaft stiffness of screw and nut cause different deformations of shaft sections. Thus the axial accumulative deformations of screw and nut are different. Secondly, the smaller the thread stiffness is, the more uniform the applied load is distributed over threads. Compared with screw in this example, the shaft section stiffness of nut is larger and the thread stiffness is smaller. As a result, load distribution on nut side is more uniform than that of screw side.

Comparing Figure 11(a) and (b), one can find that load distribution when PRSM is installed at the opposite ends is more uniform than that of installed at the same ends. The reason is that load distributions on nut and screw sides will affect each other. Owing to the same variation tendencies of the load distributions on screw and nut sides when PRSM is installed at the same ends, the nonuniform distribution of applied load is aggravated. So it is of great significance for PRSM to choose a suitable installation configuration.

Effect of thread form parameter

Thread form parameters of PRSM include thread angle, thread height, thread thickness, and pitch. Thread height, thread thickness, and pitch are analyzed here because thread angle is designed as 90° customarily.

Load distributions with different thread form are investigated by given the value of pitch as 0.4 mm, 0.8 mm, 1.2 mm, 1.6 mm, and 2.0 mm, the corresponding thread height is 0.19 mm, 0.38 mm, 0.57 mm, 0.76 mm, and 0.95 mm, and the corresponding thread thickness is 0.26 mm, 0.42 mm, 0.58 mm, 0.74 mm, and 0.85 mm, respectively.

As shown in Figure 12, load distributions on both screw and nut sides become more and more uniform with the decrease of pitch, thread height, and thickness. Among these thread form parameters, pitch has most important influence on load distribution. When pitch is 0.4 mm, thread loads on screw and nut sides are almost uniformly distributed. Therefore, it is feasible to apply a small thread form to obtain a uniform distribution.

Load distribution with redesigned thread form parameters

In order to improve the load distribution of PRSM under "Screw-T, Nut-T" load condition, the pitch and thread thickness of roller and nut are redesigned by the improvement approach mentioned above (refer to section "Redesign of thread form parameters"), and the values of thread form parameters are calculated again by equations (35) to (38). The new obtained parameters are listed in Table. 3.

Load distribution of PRSM after redesign the thread parameters of roller and nut is shown in Figure 13.

As shown in Figure 13, the maximum thread load on screw side decrease from 341 N to 277 N, and the region of load sharing coefficient changes from [0.82, 1.36] to [0.94, 1.1]. The maximum thread load on nut side decrease from 273 N to 258 N, and the region of load sharing coefficient on nut side changes from [0.95, 1.09] to [0.98, 1.04], after the redesign of thread form parameters of roller and nut. Thus the improvement approach shown in Figure 10 is demonstrated to be effective to make the applied load distribute more uniformly when PRSM is under the load condition of "Screw-T, Nut-T". Besides, even though the axial accumulative deformations of shaft sections of screw and nut have remarkable influence on load distribution, they are much smaller compared with the size of structural parameters of PRSM. Hence the differences among the pitches of screw, roller, and nut after the redesign of thread form parameters are very small. Actually these differences can only be achieved through the control of tolerance. And the manufacturing error should also be strictly controlled to ensure the expected contact conditions.

Conclusions

A model for calculating the load distribution over threads of PRSM is proposed in this paper based on the shaft section stiffness, thread stiffness and contact stiffness, and the model is verified by comparing with existed one. Some conclusions are drawn as follows:

1. The distribution of applied load over threads of PRSM basically depends on the installation configuration, material parameters and structural parameters of the screw, roller, and nut. So it is necessary for a good design parameters to acquire the uniform load distribution of PRSM.
2. The load distribution of PRSM supported at the opposite ends is more uniform than that of supported at the same end. Furthermore, the load distributions are the same under different load conditions of the same installation configuration. Furthermore, load distributions on nut and screw side will interact each other.
3. The load distribution of PRSM becomes more non-uniform with the increase of pitch and it becomes more uniform with the decrease of thread stiffness.
4. In order to obtain a uniform load distribution over the threads of PRSM, by applying the improvement approach proposed, it is feasible to slightly adjust the pitch and thread thickness of roller and nut to change the contact conditions among screw, roller and nut. The improvement approach is proved to have great benefit to improve the load distribution of PRSM.

Declaration of Conflicting Interests

The author(s) declared no potential conflicts of interest with respect to the research, authorship, and/or publication of this article.

Funding

The author(s) disclosed receipt of the following financial support for the research, authorship, and/or publication of this article: This study was funded by the National Natural Science Foundation of China (Grant No. 51275423), Specialized Research Fund for the Doctoral Program of Higher Education (Grant No. 20126102110019), the 111 Project (Grant No. B13044), China Postdoctoral Science Foundation funded project (Grant No. 2014M552483), and the Fundamental Research Funds for the Central Universities (Grant No. 3102014ZD0035).

References

1. Wang H, Tong M and Zheng P. Research on contact strength between roller screw pair on hoisting mechanism applied in deep sea crane. In: *The 3rd international conference on applied mechanics, materials and manufacturing*, 2013, pp.2001–2005.
2. Schinstock DE and Haskew TA. Dynamic load testing of roller screw EMAs. In: *Proceedings of the 31st intersociety energy conversion engineering conference (IECEC)*, vol. 1, 1996, pp.221–226.
3. Pajak M. Machine elements. To innovative production presses via roller screw planetary drives. *Konstruktion* 2010; 1–2: 24–25. ((in German).
4. Yukio O, Aron A, Miiller J, et al. Control system modification of an electromechanical pulsatile total artifical heart. *Thoughts Prog* 1997; 21: 1308–1311.
5. Jin Q, Yang J and Sun J. Motion characteristics and parameters choosing of planetary roller screw. *Manuf Technol Mach Tool* 1998; 5: 13–15.
6. Sokolov PA, Sorokin FD, Ryakhovsky OA, et al. Kinematics of planetary roller screw mechanisms. Vestnik MGTU, Mashinostroeniya 1, 2005, pp.3–14 (in Russian).
7. Ma S, Liu G, Zhou J, et al. Optimal design and contact analysis for planetary roller screw. *Appl Mech Mater* 2011; 86: 361–364.
8. Ma S, Liu G, Tong R, et al. Finite element analysis of axial elastic deformation for planetary roller screw. *J Mech Transm* 2012; 36: 78–81.
9. Zhang X, Liu G, Ma S, et al. Study on axial contact deformation of planetary roller screw. *Appl Mech Mater* 2012; 155–156: 779–783.

10. Hojjat Y and Mahde Agheli M. A comprehensive study on capabilities and limitations of roller-screw with emphasis on slip tendency. *Mech Mach Theory* 2009; 44: 1887–1899.
11. Lemor PC. The roller screw, an efficient and reliable mechanical component of electro-mechanical actuators. In: *Proceedings of the 31st intersociety energy conversion engineering conference (IECEC)*, 1996.
12. Velinsky SA, Chu B and Lasky TA. Kinematics and efficiency analysis of the planetary roller screw mechanism. *Mech Des* 2009; 131: 1–8.
13. Ma S, Liu G, Tong R, et al. A new study on the parameter relationships of planetary roller screwsMath Prob Eng 2012. DOI: 10.1155/ 2012/ 340437.
14. Jones MH and Velinsky SA. Kinematics of roller migration in the planetary roller screw mechanism. *J Mech Des* 2012; 134: 1–6.
15. Jones MH and Velinsky SA. Contact kinematics in the roller screw mechanism. *J Mech Des* 2013; 135: 1–10.
16. Sokolov PA, Sorokin FD, Ryakhovsky OA, et al. Force between working surfaces of the thread turns of a planetary roller–screw mechanism. Vestnik MGTU, Mashinostroeniya, 2006, pp.61–72 (in Russian).
17. Ma S, Liu G, Tong R, et al. A frictional heat model of planetary roller screw mechanism considering load distribution. *Mech Based Des Struct Mach* 2015; 43: 164–182.
18. Yang J, Wei Z, Zhu J, et al. Calculation of load distribution of planetary roller screws and static rigidity. *J Huazhong Univ Sci Technol* 2011; 39: 1–4.
19. Ryś J and Lisowski F. The computational model of the load distribution between elements in planetary roller screw. In: *9th International conference on fracture & strength of solids*, 2013.
20. Jones MH and Velinsky SA. Stiffness of the roller screw mechanism by the direct method. *Mech Based Des Struct Mach* 2014; 42: 17–34.
21. Yamamoto S. *Theory and calculation of screw thread connection* (K.Q. Guo, Trans.). Shanghai: Shanghai Science and Technology Literature Press, 1984, pp.45–49 (In Chinese).
22. Johnson K. *Contact mechanics*. Cambridge: Cambridge University Press, 1985, pp.84–104.
23. Harris TA and Kotzalas MN. *Essential concepts of bearing technology*. 5th ed. New York: Taylor & Francis, 2006, pp. 112–114(Rolling bearing analysis).

Appendix

Notation

a	root width of thread form
A	minimum cross-sectional area of shaft
b	thread thickness
c	crest width of thread form
d	nominal diameter
d_p	effective external diameter of external thread or effective internal diameter of internal thread
D_0	external diameter of hollow cylinder as which the internal thread is identified
e_S	thread thickness of screw
e_R	thread thickness of roller
E	Young's modulus of material
$\mathbf{f}$	vector of thread load
F_a	axial component of thread load
$F_{applied}$	applied load shared on rollers of PRSM
F_n	normal thread load
F_{NRi}	axial component of thread load on the i-th thread couple on nut side
F_{NSi}	axial load on the i-th shaft section of nut
F_r	radial component of thread load
F_{RSi}	axial load on the i-th shaft section of roller
F_{SRi}	axial component of thread load on the i-th thread couple on screw side
F_{SSi}	axial load on the i-th shaft section of screw
h_f	addendum of thread form
k_{XS}	shaft section stiffness of X
k_{XT}	thread stiffness of X
k_{XRC}	contact stiffness of threads between roller and screw or nut
$\mathbf{K}$	matrix that present deformation compatibility relationship
$\mathbf{m}_{1\times n}$	vector that all elements are 1
n	number of roller threads
$\mathbf{n}_{1\times n}$	vector that all elements are 0
$\mathbf{o}_{1\times(2n-2)}$	vector that all elements are 0
P	nominal value of pitch of thread
X	subscript that denotes the associated component as S, R, or N for screw, roller, or nut, respectively
z	number of rollers
α_R	helical angle of roller thread
δ^*	contact parameter relates to $\Sigma\rho$
δ_1	bending deformation of thread
δ_2	shear deformation of thread
δ_3	deformation of thread caused by root incline
δ_4	deformation of thread caused by root shear
δ_5	deformation of thread caused by the radial component of thread load
δ_{5-e}	deformation of external thread caused by the radial component of thread load
δ_{5-i}	deformation of internal thread caused by the radial component of thread load
δ_{XT}	total axial deformation of thread of X
$\delta_{XRC\text{-}normal}$	contact deformation in normal direction
$\delta_{XRC\text{-}axial}$	axial component of contact deformation
δ_{ave}	axial component of contact deformation under average thread load
δ_{act}	axial component of contact deformation under actual thread load
Δl_{SSi}	axial deformation of the i-th shaft section of screw

Δl_{NSi}	axial deformation of the i-th shaft section of nut
Δl_{RSi}	axial deformation of the i-th shaft section of roller
Δl_{XTi}	axial deformation of the i-th thread of X
Δl_{XRCi}	axial component of contact deformation of the i-th thread couple
$\Delta l_{sum\text{-}S}$	axial accumulative deformation at the first thread of screw
$\Delta l_{sum\text{-}R}$	axial accumulative deformation at the first thread of roller
$\Delta l_{sum\text{-}N}$	axial accumulative deformation at the first thread of nut
ε_R	difference between pitches of roller and screw
ε_N	difference between pitches of nut and roller
μ	Poisson's ratio of material
$\Sigma\rho$	summation of curvatures of two contact surfaces
Σl_{Ni}	total axial deformation within the i-th shaft section of nut
Σl_{Ri}	total axial deformation within the i-th shaft section of roller
θ	thread angle
ξ	clearance between first thread couple of screw and roller